

(Supplementary Methods online). The conventional experiment showed a typical arginine-to-proline conversion rate of ~30–40% of all proline-containing peptides (Fig. 1a,b), comprising about half of the identified peptides (Supplementary Discussion). When we grew hESCs in the conversion-tolerant light medium, the ratio between light and heavy peptides without proline was unaffected (Fig. 1c,d), but progressively changed with increasing numbers of prolines in the peptide (Fig. 1 and Supplementary Fig. 4 online). When we grew hESCs in the conversion-tolerant light medium, the first monoisotopic peak in the spectrum of the light peptide (containing [ $^{15}\text{N}_4$ ]-arginine and [ $^{15}\text{N}_1$ ]-proline) was reduced by ~30% owing to the presence of [ $^{15}\text{N}_4$ ]-arginine-derived [ $^{15}\text{N}_1$ ]-proline (Fig. 1d). This was manifested as an increase in the height of the second peak in the same spectrum (containing [ $^{15}\text{N}_4$ ]-arginine and [ $^{15}\text{N}_1$ ]-proline). As expected, the first peak in the peptide spectrum of the heavy peptide (containing [ $^{13}\text{C}_6,^{15}\text{N}_4$ ]-arginine and [ $^{13}\text{C}_5,^{15}\text{N}_1$ ]-proline) was similarly reduced upon conversion of [ $^{13}\text{C}_6,^{15}\text{N}_4$ ]-arginine to [ $^{13}\text{C}_5,^{15}\text{N}_1$ ]-proline (Fig. 1d). Notably, the same ratio measured for peptides from the light and heavy samples was consistent (Fig. 1c), also for peptides containing more than one proline (Supplementary Fig. 4). Therefore, substitution of normal arginine by [ $^{15}\text{N}_4$ ]-arginine in the light condition allowed accurate quantitation of peptide ratios.

We tested several alternative strategies of labeling these hESCs, which are notoriously sensitive to environmental changes, for accurate SILAC-based quantitation without success (Supplementary Discussion). Substitution of normal arginine by [ $^{15}\text{N}_4$ ]-arginine in the light condition provides an efficient means to quantify peptide ratios, even in cells with high conversion rates and in data sets of increased complexity because of partial conversion of arginine. We believe that these advantages outweigh the costs of using additional isotope labels and that this method extends the applicability of SILAC to cells that would otherwise be inaccessible for proper protein quantitation.

Note: Supplementary information is available on the Nature Methods website.

Dennis Van Hoof<sup>1,2,5</sup>, Martijn W H Pinkse<sup>2,4,5</sup>, Dorien Ward-Van Oostwaard<sup>1</sup>, Christine L Mummery<sup>1,3</sup>, Albert J R Heck<sup>2</sup> & Jeroen Krijgsveld<sup>2</sup>

<sup>1</sup>Hubrecht Institute, Uppsalalaan 8, 3584 CT Utrecht, The Netherlands.

<sup>2</sup>Department of Biomolecular Mass Spectrometry, Bijvoet Center for Biomolecular Research and Utrecht Institute for Pharmaceutical Sciences, Utrecht University, Sorbonnelaan 16, 3584 CA Utrecht, The Netherlands.

<sup>3</sup>Interuniversity Cardiology Institute of the Netherlands, and Heart Lung Institute, Universiteitsweg 98, 3584 CG Utrecht, The Netherlands. <sup>4</sup>Present address: Analytical Biotechnology, Delft University of Technology, Julianalaan 67, 2628 BC Delft, The Netherlands.

<sup>5</sup>These authors contributed equally to this work.

e-mail: j.krijgsveld@uu.nl

#### COMPETING INTERESTS STATEMENT

The authors declare no competing financial interests.

- Ong, S.E. & Mann, M., *Nat. Proto.* **1**, 2650–2660 (2007).
- Ibarrola, N. *et al. Anal. Chem.* **75**, 6043–6049 (2003).
- Hwang, S.I. *et al. Mol. Cell. Proteomics* **5**, 1131–1145 (2006).
- Ong, S. E., Kratchmarova, I., & Mann, M., *J. Proteome. Res.* **2**, 173–181 (2003).
- Scott, L., Lamb, J., Smith, S. & Wheatley, D.N. *Br. J. Cancer* **83**, 800–810 (2000).
- Gruhler, A. *et al. Mol. Cell. Proteomics* **4**, 310–327 (2005).
- Van Hoof, D. *et al. Expert Rev. Proteomics* **3**, 427–437 (2006).

## New lasers for flow cytometry: filling the gaps

**To the editor:** Flow cytometers rely almost exclusively on lasers for excitation of fluorescent probes. Although lasers are excellent excitation sources, their discrete wavelengths limit the visible light that is available for fluorophore excitation. Even the most modern cytometers typically provide no more than four laser wavelengths, with the traditional blue-green (488 nm) and red (633–640 nm) wavelengths being the most common. Even with multilaser instruments, coverage of the spectrum is incomplete, with gaps that exclude many useful fluorophores. This is largely due to the limited selection of wavelengths available with existing laser technology.

Two advances can eliminate these gaps. First, new diode-pumped solid state lasers provide a variety of discrete laser lines applicable for flow cytometry. Green (532 nm) and yellow-green (561 nm)

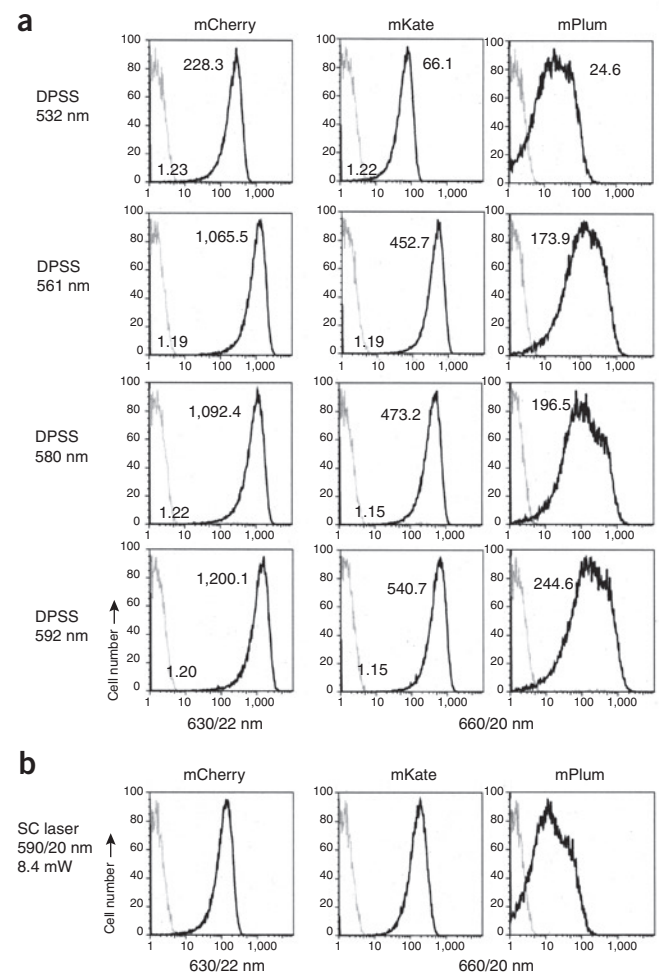


**Figure 1** | Excitation with DPSS and supercontinuum laser sources. (a) Flow cytometric analysis of mCherry, mKate or mPlum expression in *Escherichia coli* using DPSS 532, 561, 580 or 592 nm lasers, all emitting at 50 mW. Untransfected (gray) and RFP expressing cells (black) are shown in each histogram, with mean fluorescence intensities given for each peak. (b) Flow cytometric analysis of mCherry, mKate or mPlum expression using a supercontinuum white laser source, with an interposed 590/20 nm bandpass filter.

lasers are becoming common in cytometers<sup>1</sup>. Improvements in cavity design and doping increase this range even further toward orange (580–610 nm) and below 488 nm. Fiber lasers, in which a fiber optic constitutes the lasing cavity, have also increased the range of solid-state sources. Second, supercontinuum white lasers emit continuously from the violet to the infrared, allowing selective filtering of particular wavelength ranges. Examples of these technologies include DPSS 580 and 592 nm orange fiber lasers (MPB Communications, Inc.) and a supercontinuum white laser (Fianium, Ltd.; **Supplementary Fig. 1** online). These provide wavelengths that are difficult to produce using traditional technologies.

Yellow-orange laser emission (570–610 nm) is difficult to generate using lasers practical for cytometry, yet would be useful for the excitation of many fluorescent probes, such as Texas red (excitation wavelength ( $\lambda_{\text{Ex}}$ ) = 595 nm, emission wavelength ( $\lambda_{\text{Em}}$ ) = 615 nm). Long-wavelength red fluorescent proteins (RFPs) such as mCherry ( $\lambda_{\text{Ex}}$  = 587 nm,  $\lambda_{\text{Em}}$  = 610 nm), mKate ( $\lambda_{\text{Ex}}$  = 588 nm,  $\lambda_{\text{Em}}$  = 635 nm) and mPlum ( $\lambda_{\text{Ex}}$  = 590 nm,  $\lambda_{\text{Em}}$  = 649 nm) are also optimally excited in the yellow-orange range, and the search for even longer wavelength RFPs would be greatly facilitated by lasers in this range<sup>2,3</sup>.

We integrated DPSS fiber 580 and 592 nm lasers into a BD Biosciences LSR II flow cytometer (**Supplementary Fig. 1**), where they provided optimal excitation of bacteria expressing mCherry, mKate or mPlum (**Fig. 1a**). Sensitivity using the 592 nm source in particular was an improvement over 532 nm. Excitation and detection with the 561 nm laser was adequate, but occurred in the ‘tails’ of the RFP excitation spectra, rather than at the excitation maxima; this might give acceptable results for strong fluorescence emission, but would reduce sensitivity for very weak fluorescence signals. Matching the excitation maxima to the laser emission provides the best overall detection sensitivity.

Similarly, we incorporated a supercontinuum source into the same cytometer, with a 590/20 nm (580–600 nm window) filter interposed in the beam (**Fig. 1b**). This source also provided good excitation of fluorescent proteins, albeit with lower power. Although supercontinuum sources could in theory provide a single source for all laser lines, their limited power (~2 mW/nm) does not yet allow them to completely replace single-wavelength sources, which have higher power. Together, these two technologies begin to close the gaps in excitation, allowing virtually any fluorophore to be analyzed by flow cytometry.

Note: Supplementary information is available on the Nature Methods website.

**Veena Kapoor<sup>1</sup>, Fedor V Subach<sup>2</sup>, Vladimir G Kozlov<sup>3</sup>, Anatoly Grudinin<sup>3</sup>, Vladislav V Verkhusha<sup>2</sup> & William G Telford<sup>1</sup>**

<sup>1</sup>Experimental Transplantation and Immunology Branch, National Cancer Institute, National Institutes of Health, Bethesda, Maryland 20892, USA. <sup>2</sup>Department of Anatomy and Structural Biology, Albert Einstein College of Medicine, Bronx, New York 10461, USA. <sup>3</sup>Fianium Ltd., 20 Compass Point, Ensign Way, Southampton, SO31 4RA, UK.  
e-mail: telfordw@mail.nih.gov

#### COMPETING INTERESTS STATEMENT

The authors declare competing financial interests: details accompany the full-text HTML version of the paper at <http://www.nature.com/naturemethods/>.

1. Telford, W.G. *et al. Cytometry* **68A**, 36–44 (2005).
2. Shaner, N.C. *et al. Nat. Methods* **2**, 905–909 (2005).
3. Verkhusha, V.V. *et al. Nat. Biotechnol.* **22**, 289–296 (2004).

## SNPs matter: impact on detection of differential expression

**To the editor:** With the recent completion of the Perlegen–US National Institute of Environmental Health Sciences mouse resequencing project<sup>1</sup>, which adds 8 million single nucleotide polymorphisms (SNPs) to the more than 2 million SNPs already in the public databases, the genome-wide knowledge of variation among 16 of the most widely used mouse strains has increased dramatically. Given the proliferation of mouse genetic models (for example, knockout and transgenic models, selectively bred lines, heterogeneous stocks derived from standard inbred strains as well as wild mice) and the recent resurgence of sequence and microarray data using these models, we are now in a position to determine the impact of naturally occurring genetic polymorphisms on hybridization-based techniques.

As a first example, we demonstrated the impact of SNPs on detection of differential expression in the two most commonly used inbred mouse strains, C57BL/6J (B6) and DBA/2J (D2) strains (**Supplementary Methods** online). Nearly 4 million SNPs have been identified between these two strains, which is a lower-bound estimate because sequencing of only the B6 strain has been completed. We focused on the oligonucleotide microarray (in this study, Affymetrix MOE 430 2.0) as it is one of the most commonly used platforms for estimating expression. We compared two normalization methods: Affymetrix Microarray Suite 5 (MAS5) and Robust Multichip Analysis (RMA) to determine the impact of low-level analysis (**Supplementary Methods**).

We determined what percentage of the array was impacted by known polymorphisms. Overlay of all known B6 versus D2 SNPs identified 13,292 probes on the array that spanned at least one SNP and affected 6,590 probe sets (~16% of the array). Examination of the probe sets impacted by SNPs allowed us to estimate the proportion of false positives and false negatives (**Supplementary Table 1** online). We compared the candidate differentially expressed transcripts identified with and without masking SNP-affected probes, and determined whether choice of normalization algorithm reduced the impact of the SNPs (**Supplementary Data 1** and **2** online). Using MAS5 and RMA, we estimated false positive rates at the transcript level of 36 and 22%, and false negative rates of 13 and 12%, respectively (**Supplementary Table 2** online, see **Supplementary Methods** for definitions). This represented a dramatic lack of concordance in differential expression results simply owing to the presence of SNP(s). A striking illustration of an SNP-induced false negative occurred for *Acp2* (**Fig. 1**). When the microarray probe set (1427943\_at) was masked for SNPs, evidence for differential expression (a B6/D2 mRNA expression ratio) reversed direction and became significant ( $q = 3.5 \times 10^{-3}$ ; see **Supplementary Methods** for definition of  $q$ -values) (**Supplementary Table 3** online), and we confirmed this using quantitative real-time PCR. The number of SNPs impacting transcripts varied greatly: some false positive results were due to only 1 SNP impacting a probe set (*Mmd*; **Supplementary Fig. 1** online) or were the result of up to 61 transcript-level SNPs affecting all of the probe sets for a gene (*Atp1a2*; **Supplementary Fig. 2** online).

The pronounced impact of naturally occurring allelic variation on estimates of gene expression in mammals has serious